Non-linear interaction of dislocation pile-ups with ultrasonic stress waves

1991 J. Phys.: Condens. Matter 3 9351

(http://iopscience.iop.org/0953-8984/3/47/008)

J. Phys.: Condens. Matter 3 (1991) 9351–9362. Printed in the UK

Non-linear interaction of dislocation pile-ups with ultrasonic stress waves

C E Bottani†‡, P Cavassi† and P Pisani†

† Dipartimento di Ingegneria Nucleare del Politecnico di Milano, 20133 Milano, Italy

Received 21 March 1991, in final form 21 June 1991

Abstract. Non-linear ultrasound absorption in solids is mainly attributed to the depinning of dislocations from pinning points. Confirming the validity of this hypothesis we introduce here a further different non-linear mechanism associated with the release of dislocation pile-ups in polycrystalline materials. Pile-up dislocation dynamics under the action of ultrasonic stress waves has been computed by numerically solving the equations of motion of a population of interacting dislocations initially confined in a crystal grain with low-angle boundaries. Dissipated power and microscopic dynamic stress–strain cycles have then been computed together with the dependence of local critical resolved shear stress on excitation frequency and amplitude. The dissipated power plots against frequency characteristics show both regular collective dislocation effects and irregular single dislocation effects such as peaks. This last result could make possible quantitative non-destructive inspection of microstructural properties by means of a new interpretation of ultrasound attenuation measurements whenever pile-up dislocations are thought to be present.

1. Introduction

In the field of low-temperature small plastic deformations of crystals and polycrystals there are no generally accepted constitutive equations which link together strains, stresses and temperature [1]. The only exception is found in the fairly sophisticated physics of two-dimensional crystals where edge dislocations are *thermodynamic* vector point defects and stress–strain characteristics can be deduced from true equations of state [2].

Thus, in the less academic three-dimensional case, one needs to acquire specific microstructural information about specific crystalline materials in which the non-linear hereditary properties are revealed in connection with the intrinsic thermodynamic irreversibility.

Furthermore as it is difficult, although not impossible, to understand the microscopic dynamics of lattice defects by means of direct measurements [3], computer simulations have, for many years, been extensively used, in particular when referring to the theory of dislocations and when using molecular dynamics-like methods [4–9].

A stimulating, alhough very peculiar, problem in the field of the dynamic plastic response of crystals and polycrystals is constituted by the experimental evidence of plastic deformation produced by high-power ultrasonic waves. Controversy already

‡ cINFM Unità di ricerca Milano Politecnico, 20133 Milano, Italy.

0953-8984/91/479351+12$03.50

exists about *heat* generated in solids by high-power ultrasound [10, 11]. More recently, experimental evidence from synchrotron white beam x-ray diffraction topography, has revealed permanent deformations produced in aluminum single crystals by ultrasound [12] and, similarly, in large-grained zinc, by means of infrared imaging [12]. Despite these last results and many existing practical applications of high-power ultrasound for mechanical deformation and stress relieving [13], '*no satisfactory theoretical treatment explaining the interaction of high-power ultrasound with metals has appeared*' [12].

As one among the several physical models needed to explain these and related phenomena we have studied the non-linear dynamic response of a discrete dislocation pile-up, confined on a certain glide plane in a grain of a three-dimensional crystal, to ultrasonic stress waves. In this way the possible release motion [14] of 'long' straight dislocation segments in a population of strongly interacting entities of the same species has been considered putting to one side the depinning instability of 'short' isolated segments interacting with the external field only which had been treated already (see e.g. [15, 16]).

To illustrate the matter we refer to a crystal grain whose *small angle boundaries* consist of walls of plane parallel edge dislocations whose number density is less than one per lattice spacing [17]: in between the two parallel borders we imagine a system of N straight infinite positive edge dislocations, each parallel to the borders, able to move on a unique crystallographic glide plane. We assume that no wall dislocations lie on this plane.

Under these assumptions the only significant independent variables are the positions of the dislocations on the glide plane, and the problem becomes one-dimensional. We disregard interactions with dislocations lying on other glide planes: the results we obtained were still comparable with those inferred from experimental evidence, provided the host crystal is not too work-hardened [18].

Moreover we suppose that we are far from the melting temperature and that thermal fluctuations are negligible [19, 20]. The main causes of dislocations slowing down in a perfect crystal are the dissipative interactions with both the phonon and electron subsystems. These mechanisms originate viscous forces proportional to the dislocation velocities [21].

As a final assumption we neglect the effective mass of the dislocations: in fact inertial effects are small if compared with viscous ones when glide *rigid* motion, and *not vibrational* motion, of pinned dislocation segments is considered [22].

Using a computer we solved the equations of discrete dislocation dynamics and obtained detailed information about the positions, velocities, linear density of dislocations in the crystal, and therefore dissipated power, strains and strain rates as functions of such parameters as the number of dislocations, crystal dimensions, frequency and the amplitude of the external stress wave.

The behaviour of a crystal grain undergoing a sinusoidal stress wave has been examined, by making an analysis in terms of frequency and amplitude. In this way it has been possible to simulate novel amplitude dependent (non-linear) ultrasonic absorption in matter by dislocations not related to the mechanism of depinning [16].

2. Dynamics of dislocations

As is well known, the internal forces (per unit length) acting between two parallel infinite edge dislocations are tensorial: they depend both on distance between dislocation lines and angle between Burgers vectors even in an elastically isotropic medium.

Let the glide planes be parallel to the (xz) plane and the z-axis be parallel to the dislocation lines. If a dislocation line coincides with the z-axis and another one passes through the point (r,θ) on the plane (xy), then the x component of the *configurational* internal force (per unit length) acting on the dislocation at (r,θ) is [17]

$$F_x = \frac{\mu b_1 b_2}{2\pi(1-\nu)} \frac{\cos\theta \cos 2\theta}{r}. \tag{1}$$

In the case of two dislocations laying on the same glide plane, the first at x_1 and the second at x_2, $(\theta = 0)$, we have

$$F_x = \frac{\mu b_1 b_2}{2\pi(1-\nu)} \frac{1}{(x_1 - x_2)}. \tag{2}$$

We now consider two walls at $x = -d$ and $x = +d$, perpendicular to the glide plane, with length $2L$: the force $bS_0(x)$ exerted by the walls on a dislocation at x is [17]:

$$bS_0(x) = N_s \frac{\mu b b_s}{2\pi(1-\nu)} \left[\frac{x+d}{(x+d)^2 + L^2} + \frac{x-d}{(x-d)^2 + L^2} \right]. \tag{3}$$

N_s representing the number of dislocations in each wall, with $N_s/2L \ll 1$ and b_s the Burgers vector of *sessile* wall dislocations and b the Burgers vector of glide dislocations. Figure 1 shows the shear field $\sigma_{yx}(x,0) = S_0(x)$ produced by the walls on the glide plane $y = 0$ (in non-dimensional units) and figure 2 the corresponding *potential* well $U_0(x) = -\int_{-d}^{x} S_0(x)\,dx$. Because of the logarithmic divergence of the dislocation–dislocation potential energy (see equation (1)) it is not possible here to assume a null potential energy at infinity.

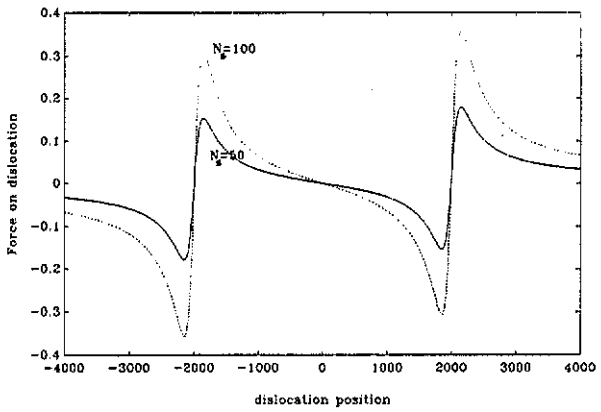

Figure 1. The force exerted on a positive glide dislocation by two parallel grain boundary walls (see equation (3)).

The dynamics of pile-up dislocations is described by a system of ordinary differential equations (see e.g. [22]) of a dissipative nature:

$$B\frac{dx_i}{dt} = bS_0(x_i) - \frac{\mu b^2}{2\pi(1-\nu)} \sum_{j \neq i} \frac{1}{x_j - x_i} + b\tau_{yx}(x,t) \qquad (i,j = 1,N) \tag{4}$$

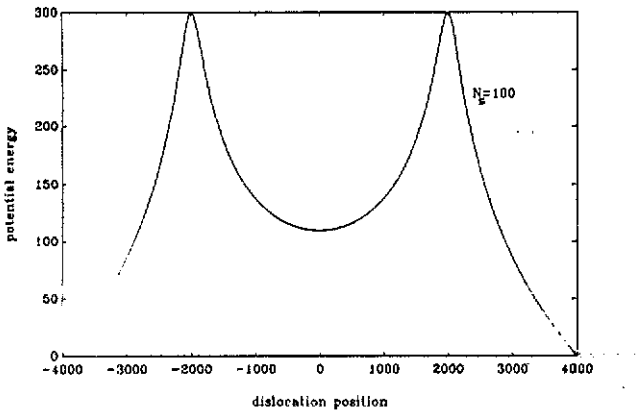

Figure 2. The elastic potential energy well corresponding to the force field of figure 1.

where τ_{yx} is an additional external stress field superimposed on $S_0(x)$, N is the number of pile-up dislocations on the considered glide plane and B is the dislocation drag coefficient connected mainly to dislocation–phonon and dislocation–electron scattering [16, 21].

Equation (4) is just a *quasi-static* force balance: no inertial effects have been included as discussed in the introduction. Should one wish to consider such inertial effects it would not be sufficient just to add to (4) a term proportional to dislocation acceleration: for a thorough discussion of such corrective terms in (4) see [22]. In the initial part of our work we took pure acceleration terms [22] into account and obtained, in all cases illustrated here, results not significantly different from those obtained without them: thus we shall not mention inertial effects anymore.

We now introduce non-dimensional time, length and shear scales but, for the sake of simplicity, we shall retain the old symbols of equation (4):

$$\frac{\mathrm{d}x_i}{\mathrm{d}t} = S_0(x_i) - \sum_{j \neq i} \frac{1}{x_j - x_i} + \tau(x,t) \qquad (i,j = 1,N). \tag{5}$$

We can recover physical quantities by multiplying x by b, t by $B2\pi(1-\nu)/\mu$, and τ by $\mu/2\pi(1-\nu)$.

For equation (4) to be valid all dislocation velocities must be less than the shear sound velocity in the medium [22]. In particular in the initial positions the dislocation velocities (maximum velocities in a relaxation without external stress) must satisfy this requirement. In all the simulations described later the initial velocities were exactly zero corresponding to the initial equilibrium positions previously found solving (4) with a *reasonable* distribution of initial positions and putting the external stress τ equal to zero: the *unforced* asymptotic solutions of (4) were taken as good equilibrium initial positions for subsequent *forced* tests (see next section).

3. Response to monochromatic stress waves

Let us now examine the behaviour of dislocations while being subjected to ultrasonic stress waves. This was simulated by putting the expression:

$$\tau(x,t) = \tau_0 \sin(kx - \omega t) \tag{6}$$

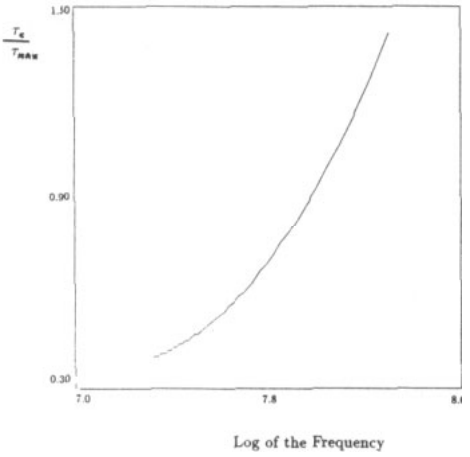

Figure 3. Dynamic critical resolved shear stress (in units of maximum grain boundary stress, see text) against stress wave frequency.

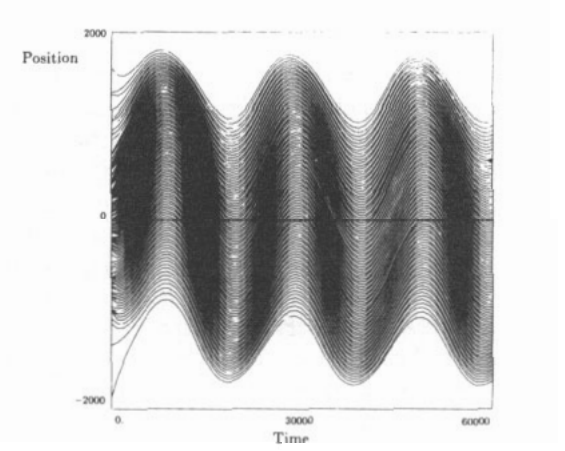

Figure 4. Dislocation positions as functions of non-dimensional time under the action of a monochromatic stress wave for a subcritical amplitude $\tau_{max}/2$: all dislocations remain confined in the grain.

in equation (5) for the external shear stress resolved on the glide plane. For all dislocations inside the grain to experience the same field simultaneously, the wavelength of the exciting wave must be much greater than the distance between the walls, as expressed by the inequality: $\lambda = 2\pi/k \gg 2d$.

For instance, setting $d = 2000$ and taking for the sound velocity in the crystal $v_t = \sqrt{\mu/\rho} \simeq 3000\ \mathrm{m\,s^{-1}}$, we get $\nu = \omega/2\pi \ll 1.9$ GHz.

We see that, within the ultrasonic frequency spectrum, we can safely neglect the spatial dependence in (6), and use the simplified form:

$$\tau(t) = \tau_0 \sin(\omega t). \tag{7}$$

3.1. Dynamic critical resolved shear stress

First of all we determined the *dynamic critical shear* $\tau_0 = \tau_c$, that is the maximum value of the amplitude of the external stress wave below which all forced dislocations remain confined inside the grain and only oscillate about equilibrium positions (linear *anelastic* response) and above which deconfinement motion starts (non-linear *viscoplastic* response). Anelastic response is reversible in terms of the purely mechanical motion of dislocations but not in thermodynamical terms, leading to ultrasound absorption and crystal heating, while viscoplastic response is irreversible from all points of view.

In figure 3 the behaviour of critical shear τ_c (in units of maximum grain boundary shear $\tau_{max} = S_{0max}$) is represented as a function of ultrasound frequency for $N = 100, d = 2000, L = 150$ and $N_s = 100$. The expression for τ_{max} is obtained from equation (3) and is

$$\tau_{max} = N_s \frac{\mu b_s}{2\pi(1-\nu)} \left[\frac{2d}{(2d)^2 + L^2}\right] \approx N_s \frac{\mu b_s}{4\pi(1-\nu)d} \tag{8}$$

corresponding to $x = \pm d$.

We see that increasing the frequency increases critical shear, that is dislocations find it less easy to leave the grain: dislocation–dislocation internal repulsion is less effective in *helping* the external stress. In the frequency range we have explored the slope of the characteristic τ_c against frequency is ever increasing: the asymptotic high frequency behaviour of τ_c would be reached at frequencies violating the conditions outlined in section 3. The zero frequency limit of τ_c is a finite constant as can be guessed from the decreasing slope of the curve towards lower frequencies.

This critical stress behaviour is analogous to that seen in a more traditional low frequency mechanical test: although it is impossible to get a unified theory of plastic mechanical response of materials, this seems to be a characteristic feature of all deformation processes controlled by dislocation release and motion.

In figures 4 and 5 we report the positions of dislocations as functions of time during three periods of forced motion. The case relates to 100 dislocations with an excitation frequency of 50 MHz. In figure 4 the amplitude of the ultrasonic wave corresponds to $\tau_0 = \tau_{max}/2$: all dislocations remain confined inside the grain. In figure 5 the amplitude is $\tau_0 = \tau_{max}$: groups of dislocations get through the grain boundary pushed by both external shear and internal repulsion. Once the first group has abandoned the original grain the dislocation density within it is lowered, the repulsion also becomes lower and the dynamic critical shear increases: this can be seen from the less numerous dislocation groups subsequently freed. This clearly shows the strongly irreversible nature of dislocation motion even in the absence of dislocation sources and dislocation annihilation.

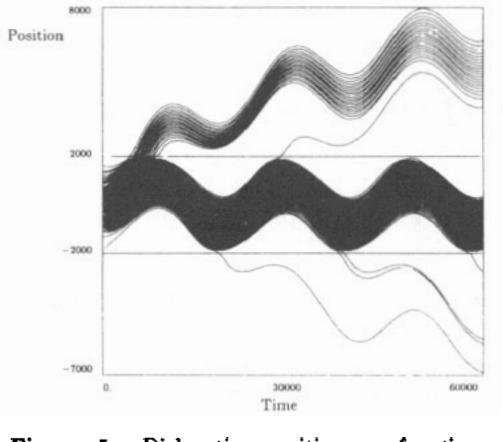

Figure 5. Dislocation positions as functions of adimensional time under the action of a monochromatic stress wave for an amplitude equal to τ_{max}: the deconfinement motion of groups of dislocations is evident.

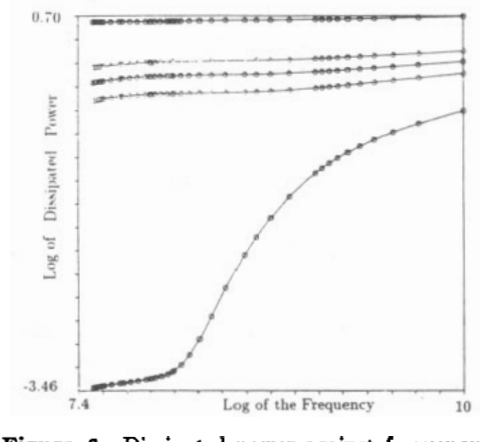

Figure 6. Dissipated power against frequency for five different stress wave amplitudes (from bottom to top: $\tau_0 = 0.01, 0.4, 0.5, 0.6, 1\ \tau_{max}$). With this representation the lowest curve shows the *typical* gross behaviour of all curves while the details of the other curves are not visible. In the low frequency region fine irregular behaviour was found at higher amplitudes (see figure 7). In figures 6, 7 and 8 power is measured in units $\mu^2 b^2/4\pi^2(1-\nu)^2 B$, see text.

3.2. Dissipated power

The energy dissipated per unit time and length during the motion of a dislocation line, that is the ***dissipated power*** per unit line, is given by

$$W = Bv^2 \tag{9}$$

where B is the dislocation drag coefficient already introduced (see [21] and equation (4)) and v is the velocity of the dislocation segment under consideration. For infinite straight dislocations v is constant along the dislocation line but varies with time as the dislocation is accelerated as a whole.

The power dissipated during the movement of dislocations concides with that part of the ultrasound power which is irreversibly absorbed by the medium; using the same non-dimensional units as in equation (5) it can be written as

$$W = \sum_{i=1}^{N} v_i^2$$

where N is the number of dislocations and v_i the speed of the ith dislocation. In this way we measure the dissipated power in units $\mu^2 b^2/4\pi^2(1-\nu)^2 B$.

The mean power dissipated in each period of the forcing stress wave (after the initial transient) can be obtained directly from our numerical data as

$$\overline{W} = \frac{1}{N_t} \sum_{j=1}^{N_t} \sum_{i=1}^{N} v_{ij}^2$$

where N = number of dislocations, N_t = number of sampling instants in each period, v_{ij} = velocity of the ith dislocation at the jth instant.

To satisfy the sampling theorem a choice of 20 points per period for the forcing sinusoid turned out to be a reasonable one in the relevant frequency spectrum.

In figure 6 the logarithm of mean dissipated power is plotted against the logarithm of the frequency at different shear amplitudes.

Several considerations are in order.

Dissipated power increases with excitation frequency but there is a tendency (this is clearly visible only in the lowest curve due to scale problems) to reach a frequency independent regime at higher frequencies; the presence of a double flex is common to all curves and there is an increase in the frequencies at which the inflexion points occur, increasing the stress wave amplitude. In general we found the foreseeable result that, at fixed frequency and dislocation number, the dissipated power increases as the square of the amplitude of the exciting stress wave.

The main feature exhibited by these curves is the fact that three different frequency regions seem to exist:

(i) a regular region with downward curvature above the second flex frequency;
(ii) a regular region with upward curvature between the two flex frequencies; and
(iii) an irregular region (with peaks) in the low frequency regime.

This last region is not visible in figure 6 but is clearly shown in an enlarged portion of the maximum amplitude curve ($\tau_0 = \tau_{max}$) reproduced in figure 7. Below some characteristic critical amplitude the irregular region is washed out in any case.

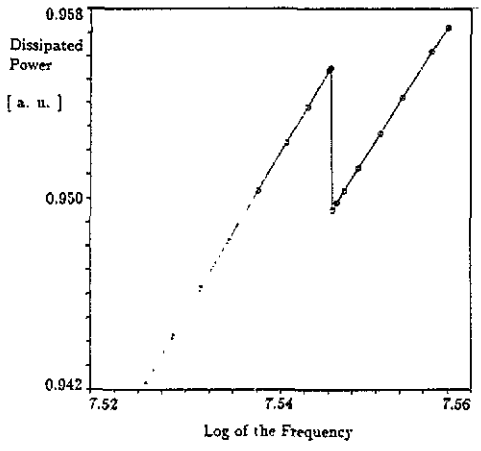

Figure 7. Sawtooth shape of dissipated power around the critical frequency at which the first dislocation overcomes the grain boundary barrier (enlarged portion of the upper curve in figure 6).

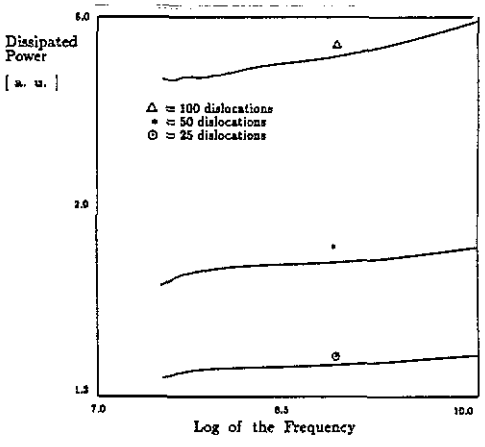

Figure 8. Dissipated power against frequency for three different dislocation numbers at constant stress wave amplitude.

The first peak (when present) encountered when decreasing the frequency corresponds to the frequency at which the first dislocation escapes from the grain. Figure 7 shows the sawtooth local structure of the dissipation curve corresponding to this phenomenon: starting at higher frequencies and decreasing the frequency we see a very sharp increase in the dissipation as the first dislocation overcomes the grain boundary barrier at a very definite frequency. At lower frequencies, however, the first curve becomes irregular because at each point it corresponds an ever increasing number of dislocations leaving the grain and the confined pile-up system is changing continuously.

Similar results are obtained with fewer dislocations at higher amplitudes and lower frequencies (see figure 8). In the case of 50 dislocations, for instance, corresponding to an amplitude $\tau_0 = \tau_{max}/2$, no dislocation can leave the grain even at the smallest frequency we considered.

4. Stress–strain characteristics

The starting point for the determination of global stress–strain characteristics in the microplastic regime is always the Orowan equation [17]

$$\dot{\varepsilon}(t) = b\rho\bar{v} \tag{10}$$

where $\dot{\varepsilon}$ is the plastic shear strain rate, ρ is the average density of mobile dislocations and $\bar{v}$ their average velocity.

To compute (10) we used the time-dependent joint distribution $N(x, v, t)$ of dislocation positions and velocities: $N(x_i, v_j, t)$ being the number of dislocations with positions between x_i and $x_i + \Delta x$ and velocities between v_j and $v_j + \Delta v$, at time t. The mean dislocation velocity (discrete) Eulerian field is then

$$\bar{v}(x_i, t) = \frac{\sum_{j=1}^{N_v} N(x_i, v_j, t) v_j}{\sum_{j=1}^{N_v} N(x_i, v_j, t)}$$

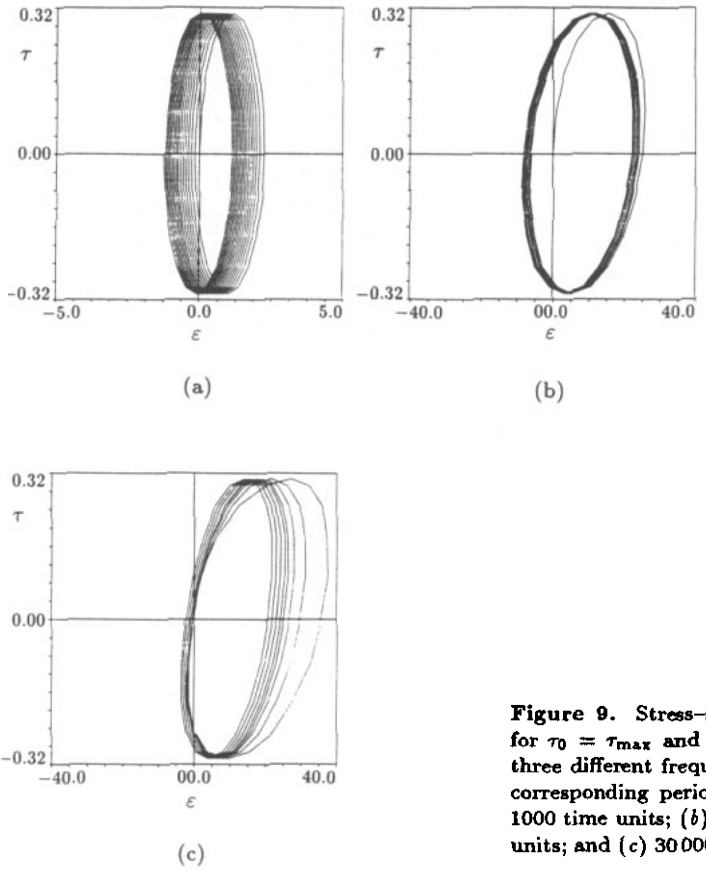

Figure 9. Stress–strain cycles for $\tau_0 = \tau_{max}$ and $N = 100$ at three different frequencies. The corresponding periods are: (*a*) 1000 time units; (*b*) 15 000 time units; and (*c*) 30 000 time units.

and the mean density of mobile dislocations is

$$\rho(x_i, t) = \frac{\sum_{j=1}^{N_v} N(x_i, v_j, t)}{\Delta x}$$

Mean (global) plastic strain rate is similarly built up as

$$\dot{\varepsilon}(t) = b \frac{1}{N_x} \sum_{i=1}^{N_x} \frac{\sum_{j=1}^{N_v} N(x_i, v_j, t) v_j}{\Delta x}. \tag{11}$$

$N(x, v, t)$ was computed by the IMSL routine BDCOU2, which constructs bidimensional istograms.

For obtaining stress–strain graphs we integrated (11) numerically to get ε and plotted τ against ε.

We have studied several cases corresponding to dislocation numbers of $N = 100, 50, 25$ and stress wave amplitudes ranging from $\tau_{max}/100$ to τ_{max}. The ultrasound frequencies were chosen in order to cover the spectrum examined so far, with particular attention being paid to the frequencies where the first dislocation leaves the grain at fixed N and τ_0.

In this way we studied frequencies ranging from 30 MHz to 1 GHz, corresponding to periods of the sinusoid ranging from 30 000 to 1000 units of our non-dimensional time.

Let us start with the case $N = 100$ and $\tau_0 = \tau_{max}$ in figure 9. It appears that the area of the first cycle grows on decreasing the frequency, that is with an increase in the period of the exciting sinusoid, while in successive cycles this effect is no longer visible; this is due to the fact that for $T = 30\,000$ many dislocations leave the grain during the first cycle (see figure 5), so that the confined system sees its population lowered in the following periods. The lower number of dislocations inside the grain makes the deformation be smaller, for the same stress. At the same time the maximum (plastic) deformation relative to the first semiperiod of the excitation increases.

In all these cases the cycles are asymmetrical, that is the positive maximum deformation at zero shear is much greater than the negative one; this is reminescent of the *Bauschinger effect* and is strictly related to this type of irreversible motions.

At high frequencies no dislocation can leave the grain; the strain cycle tends to end, recovering a certain symmetry. This means that deformation does not increase with time, and negative deformations become comparable with positive ones (transition from viscoplastic to anelastic regimes).

At low frequencies we still have a decrease in the positive maximum deformation after the first cycle but the strain cycle does not tend to end.

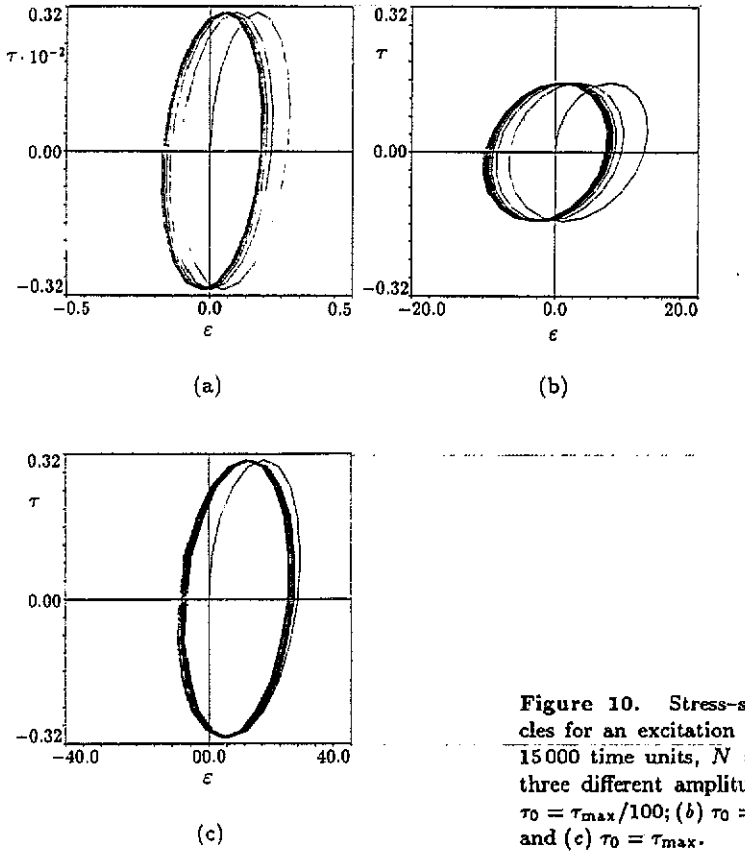

Figure 10. Stress–strain cycles for an excitation period of 15 000 time units, $N = 100$ at three different amplitudes: (*a*) $\tau_0 = \tau_{max}/100$; (*b*) $\tau_0 = \tau_{max}/2$; and (*c*) $\tau_0 = \tau_{max}$.

Let us analyse now the case with excitation period $T = 15\,000$, changing the amplitude τ_0, but always with 100 dislocations (figure 10).

For $\tau_0 = \tau_{max}/100$:

(i) the cycles quickly tend to a symmetric shape after a first asymmetric cycle; similar behaviour is found for $\tau_0 = \tau_{max}/2$;

(ii) but the asymptotic value of maximum positive plastic strain is less the the negative one; for $\tau_0 = \tau_{max}$; and

(iii) cycles remain asymmetric although they slowly become narrower.

5. Conclusions

The response of a dislocation pile-up confined in a crystalline grain with low-angle boundaries to ultrasonic monochromatic stress waves was found to be highly non-linear, showing a transition from regular stable behaviour to irregular unstable behaviour at critical amplitudes, dislocation numbers and excitation frequencies.

Coupled non-linear differential equations of dislocation dynamics have been solved, by computer, to obtain detailed information on amplitude dependent ultrasound attenuation, dynamic critical resolved shear stress of confined pile-ups and microscopic stress–strain cycles.

In contrast to previous work on discrete dislocation dynamics, here a realistic barrier stress field has been added to the dislocation mutual repulsion and viscous drag due to interactions with the host medium. In this way the feasibility of even more realistic computations, directly comparable with experimental findings, has been proved.

To this goal interaction among different glide systems and different dislocation types could be considered, at least statistically.

On the basis of our preliminary results ultrasound attenuation could be reconsidered as a powerful quantitative method to investigate specific microstructural properties of solids containing confined dislocation systems and their structural stability. Information in this area is known to be relevant to several basic and applied fields such as, for example, microcrack formation.

Acknowledgments

This work has been done under a contract between CNR and Politecnico di Milano in the frame of *Progetto Finalizzato Materiali Speciali per Tecnologie Avanzate del CNR.*

Professor F M Mazzolai is gratefully acknowledged for a discussion about possible connections with internal friction measurements.

References

[1] Gittus J and Zarka J (ed) 1986 *Modelling Small Deformations of Polycrystals* (New York: Elsevier)

[2] Bottani C E and Jacona M 1989 *J. Phys.: Condens. Matter* **1** 8337

[3] Neuhäuser H 1983 Slip-line formation and collective dislocation motion *Dislocation in Solids* vol 6, ed F R N Nabarro (Amsterdam: North-Holland) p 319

[4] Solovev V A 1972 *Phys. Met. Metallogr.* **34** 153

[5] Weertman J 1957 *J. Appl. Phys.* **28** 1185

[6] Rosenfield A R and Hahn G T 1968 *Acta Metall.* **16** 755

[7] Kanninen M F and Rosenfield A 1969 *Phil. Mag.* **20** 569
[8] Rosenfield A and Kanninen M F 1970 *Phil. Mag.* **22** 143
[9] Bassim M N, Jesser W A, Kuhlmann-Wilsdorf D and Wilsdorf H G F (ed) 1986 *Low-Energy Dislocation Structures* (New York: Elsevier)
[10] Green Jr R E 1975 *Ultrasonics* **13** 117
[11] Mignogna R B, Green Jr R E, Duke Jr J C, Henneke II E G and Reifsnider K L 1981 *Ultrasonics* **19** 159
[12] Green Jr R E 1989 *Elastic Wave Propagation* ed M F McCarthy and M A Hayes (Amsterdam: North-Holland) p 581
[13] Puskar A 1982 *The Use of High-Intensity Ultrasonics* (New York: Elsevier)
[14] Balakrishnan V and Bottani C E 1986 *Phys. Rev.* B **33** 5157
[15] Schöck G 1983 *Dislocations in Solids* vol 3, ed F R N Nabarro (Amsterdam: North-Holland) p 63
[16] Nowick A S and Berry B S 1972 *Anelastic Relaxation in Crystalline Solids* (New York: Academic) p 427
[17] Nabarro F R N 1967 *Theory of Crystal Dislocations* (Oxford: Oxford University Press)
[18] Basinski S J and Basinski Z S 1983 *Dislocations in Solids* vol 4, ed F R N Nabarro (Amsterdam: North-Holland) p 261
[19] Bottani II C E 1989 *Nuovo Cimento* D **11** 865
[20] Bottani II C E 1991 *Nuovo Cimento* D **13** 1035
[21] Alshits V I and Indenbom V L 1986 *Dislocations in Solids* vol 7, ed F R N Nabarro (Amsterdam: North-Holland) p 43
[22] Kosevich A M 1988 *Dislocations in Solids* vol 1, ed F R N Nabarro (Amsterdam: North Holland) p 33